



1 **Evidence for renoxification in the tropical marine boundary layer**

2 **Chris Reed^{1†}, Mathew J. Evans^{1,2}, Leigh R. Crilley³, William J. Bloss³, Tomás Sherwen¹,**
3 **Katie A. Read^{1,2}, James D. Lee^{1,2} and Lucy J. Carpenter¹**

4 [1] Wolfson Atmospheric Chemistry Laboratories (WACL), Department of Chemistry,
5 University of York, Heslington, York, YO10 5DD, United Kingdom

6 [2] National Centre for Atmospheric Science (NCAS), University of York, Heslington, York,
7 YO10 5DD, United Kingdom

8 [3] School of Geography, Earth and Environmental Sciences, University of Birmingham,
9 Edgbaston, Birmingham, B15 2TT, United Kingdom

10 Corresponding author: Chris Reed (chris.paul.reed@gmail.com)

11 †Now at Facility for Airborne Atmospheric Measurements (FAAM), Building 146, Cranfield
12 University, Cranfield, MK43 0AL, United Kingdom

13 **Abstract**

14 We present two years of NO_x observations from the Cape Verde Atmospheric Observatory
15 located in the tropical Atlantic boundary layer. We find NO_x mixing ratios peak around solar
16 noon (at 20-30 pptV depending on season), which is counter to box model simulations that show
17 a midday minimum due to OH conversion of NO₂ to HNO₃. Production of NO_x via
18 decomposition of organic nitrogen species and the photolysis of HNO₃ appear insufficient to
19 provide the observed noon-time maximum. A rapid photolysis of nitrate aerosol to produce
20 HONO and NO₂, however, is able to simulate the observed diurnal cycle. This would make it the
21 dominant source of NO_x at this remote marine boundary layer site overturning the previous
22 paradigm of transport of organic nitrogen species such as PAN being the dominant source. We
23 show that observed mixing ratios (Nov-Dec 2015) of HONO at Cape Verde (~2.5 pptV peak at
24 solar noon) are consistent with this route for NO_x production. Reactions between the nitrate
25 radical and halogen hydroxides which have been postulated in the literature appear to improve
26 the box model simulation. This rapid conversion of aerosol phase nitrate to NO_x changes our
27 perspective of the NO_x cycling chemistry in the tropical marine boundary layer, suggesting a
28 more chemically complex environment than previously thought.

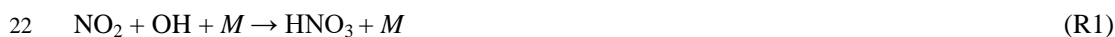


1 **1 Introduction**

2 The chemical environment in the remote marine boundary layer (MBL) is characterized by very
3 low concentrations of nitrogen oxides ($\text{NO}_x = \text{NO} + \text{NO}_2$), high concentrations of water vapour
4 and the presence of inorganic halogen compounds, resulting in net daytime ozone (O_3)
5 destruction (Dickerson et al., 1999; Read et al., 2008; Sherwen et al., 2016; Vogt et al., 1999).
6 This MBL loss of ozone plays an important role in determining the global budget of ozone and
7 the overall oxidizing capacity of the region. Understanding the concentrations of NO_x in these
8 environments is thus important for determining the global ozone budget, alongside wider
9 atmospheric chemical impacts.

10 NO_x in the remote MBL has been attributed to a) long range transport and decomposition of
11 species such as PANs, organic nitrates, or HNO_3 (Moxim et al., 1996) b) shipping emissions
12 (Beirle et al., 2004) c) a direct ocean source (Neu et al., 2008) and d) its direct atmospheric
13 transport (Moxim et al., 1996). However, more recently the possibility of ‘renoxification’ by
14 particulate nitrate photolysis has garnered attention (Baergen and Donaldson, 2013; Cohan et al.,
15 2008; Handley et al., 2007; Ndour et al., 2009; Scharko et al., 2014; Ye et al., 2016a, 2016b;
16 Zhou et al., 2003).

17 The oxidation of NO_2 to HNO_3 by OH is through the predominant sink for NO_x in the remote-
18 MBL. NO_x can also be converted into aerosol phase nitrate via the hydrolysis of N_2O_5 (R2)
19 (Evans and Jacob, 2005) but this is slow in these low NO_x environments. NO_x can be returned
20 through HNO_3 photolysis (R3) or reaction with OH (R4) but in general these processes are slow
21 and so HNO_3 can deposit to the surface, be washed out by rain, or taken up by aerosol (R5).





2 More recently the production and subsequent hydrolysis of halogen nitrates (IONO₂, BrONO₂,
3 ClONO₂) have been suggested to be a potentially important sink for NO_x in the marine boundary
4 layer (Keene et al., 2007, 2009; Lawler et al., 2009; Pszenny et al., 2004; Sander et al., 1999)

5 In this paper we investigate the budget of NO_x in the remote MBL using observations of NO_x
6 and HONO collected at the Cape Verde Atmospheric Observatory during 2014 and 2015. We
7 use a 0-D model of NO_x, HO_x, halogen, and VOC chemistry to interpret these observations and
8 investigate the role that different NO_x source and sink terms play.

9 **2 Methodology**

10 The Cape Verde Atmospheric Observatory (CVO), a global WMO Global Atmospheric Watch
11 (GAW) station, is located in the tropical North Atlantic (16.864, -24.868) on the island of São
12 Vicente and is exposed to air travelling from the North East in the trade winds (Carpenter et al.,
13 2010). In general, the air reaching the station has travelled many days over the ocean since
14 exposure to anthropogenic emissions, thus the station is considered representative of the remote
15 marine boundary layer (Read et al., 2008). A large range of compounds are measured at the
16 CVO (Carpenter et al., 2010), but we focus here on the NO and NO₂ continuous measurements,
17 alongside HONO measurements that were made for a short period in Nov/Dec 2015.

18 **2.1 NO and NO₂**

19 NO and NO₂ are measured by NO chemiluminescence (Drummond et al., 1985) coupled to
20 photolytic NO₂ conversion by selective photolysis at 385-395 nm as described by (Lee et al.,
21 2009; Pollack et al., 2011; Reed et al., 2016a, 2016b; Ryerson et al., 2000). A single
22 photomultiplier detector switches between 1 minute of chemiluminescent zero, 2 minutes of NO,
23 and 2 minutes of NO_x measurement. Calibration for NO sensitivity and NO₂ converter efficiency
24 occurs every 71 hours in ambient air; in this way correction for humidity affecting sensitivity,
25 and O₃ affecting NO₂ conversion efficiency are unnecessary. The humidity of the sample gas
26 reduced by a Nafion dryer (PD-50T-12-MKR, Permapure), fed by a constant sheath flow of zero
27 air (PAG 003, Eco Physics AG) which is also filtered through a Sofnofil (Molecular Products)



1 and activated carbon (Sigma Aldrich) trap. This zero air is also used to determine the NO₂
2 artifact signal which can arise when NO_x free air is illuminated at UV wavelengths due to
3 photolysis of HNO₃ etc., adsorbed on the walls of the photolysis cell (Nakamura et al., 2003;
4 Pollack et al., 2011; Ryerson et al., 2000). NO artifact correction is made by assuming it is
5 equivalent to a stable night-time NO value in remote regions (Lee et al., 2009), away from any
6 emission source, where NO should be zero in the presence of O₃. Reed et al., (2016b) showed
7 that thermal interferences in NO₂ using this technique may cause a bias in cold or temperate
8 remote regions, but that in warm regions, such as Cape Verde, the effect is negligible. Photolytic
9 interferences such as BrONO₂ and HONO, and inlet effects may also alter the retrieved NO or
10 NO₂ (Reed et al., 2016a, 2016b). These effects are considered to be sufficiently small that the
11 concentrations of NO and NO₂ can be determined within an accuracy of 5% and 5.9%
12 respectively (Reed et al., 2016a, 2016b) at the (very low) levels present at CVO. The instrument
13 having a zero count rate of ~ 1700 Hz with 1 σ standard deviation of that signal being ~ 50 Hz
14 this gives a precision of 7.2 pptV for 1 second data with typical sensitivity over the measurement
15 period of 6.9 cps/pptV. The resultant limits of detection for NO and NO₂ being 0.3 and 0.35
16 pptV when averaged over an hour.

17 2.2 HONO

18 Between 24th November and 3rd December 2015 a Long Path Absorption Photometer (LOPAP)
19 (Heland et al., 2001) was employed at CVO to provide an *in-situ* measurement of nitrous acid.
20 The LOPAP has its own thermostated inlet system with reactive HONO stripping to minimise
21 losses so did not sample from the main lab manifold. The LOPAP inlet was installed on the roof
22 of a container lab ~ 2.5 m above ground level, unobstructed from the prevailing wind.
23 Calibration and operation of the LOPAP was carried out in line with the standard procedures
24 described by Kleffmann and Wiesen, (2008). Further details of the HONO measurement
25 approach can be found in (Crilley et al., 2016), with the detection limit determined to be <1
26 pptV.

27 2.3 Box Model



1 We use the Dynamically Simple Model of Atmospheric Chemical Complexity (DSMACC) box
2 model (Emmerson and Evans, 2009) to interpret the observed NO_x measurements. We focus on
3 the summer season (June, July, and August) as this has the largest data coverage. The model is
4 run for day 199 at 16.864°N , -024.868°W . We initialize the model with the mean observed H_2O ,
5 CO , O_3 , VOCs (Carpenter et al., 2010; Read et al., 2012), $100 \mu\text{m}^2/\text{cm}^3$ aerosol surface area
6 (Carpenter et al., 2010). We also initialise the model with 1.5 ppt of I_2 and 2.5 ppt of Br_2 to
7 provide ~ 1.5 pptV of IO and ~ 2.5 pptV BrO during the day, consistent with the levels measured
8 over 9 months at the CVO during 2007 (Mahajan et al., 2010; Read et al., 2008). We use the
9 average diurnal cycle of the measured HONO concentrations, described above. Solar radiation at
10 this location in the tropics shows little seasonal variation, hence photolysis rates are similar in
11 summer and autumn. We assume clear sky conditions for photolysis. The unconstrained model is
12 run forwards in time until a stable diurnal cycle is attained; ~ 3 days. A full description of the
13 model chemistry is provided in the supplementary material. The base case chemistry has only
14 gas phase sources plus gas phase and deposition sinks for NO_x as described in the supplementary
15 material.

16 **3 Results and discussion**

17 **3.1 Diurnal cycles in NO_x and HONO**

18 Figure 1 shows the measured mean diurnal cycles of NO , NO_2 , NO_x , and O_3 observed in each
19 season (Meteorological Spring – Mar, Apr, May; Summer – Jun, Jul, Aug; Autumn – Sep, Oct,
20 Nov; and Winter – Dec, Jan, Feb) during 2014 and 2015. Every season shows a strong diurnal
21 cycle in NO , peaking after solar noon at around $\sim 13:00$ to $14:00$. The diurnal cycle of NO_2 is
22 much less pronounced but also exhibits weak maxima in the early afternoon. Overall this leads to
23 a maximum in NO_x during the day. This behaviour is consistent throughout the year and air
24 mass, though not necessarily on a “day-to-day” basis.

25 The observed diurnal cycle in NO_x is hard to explain with conventional chemistry. The increase
26 in night time NO_x suggests a continuous source but the maximum around noon suggests a
27 photolytic source. Given the predominant NO_x sink is reaction with OH to form HNO_3 , it would
28 be expected that there would be a minimum in NO_x during the day rather than a maximum.



1 Similar observations have been reported previously (Monks et al., 1998) at the Cape Grim
2 Baseline Air Pollution station (-40.683, 144.670), a comparably remote site in the southern
3 hemisphere, and during the Atlantic Stratocumulus Transition Experiment (ASTEX) cruise
4 (~29°N, 24°W) which reported similar daytime NO_x production (Carsey et al., 1997). The
5 observed behaviour in the CVO NO_x was historically attributed to thermal decomposition of NO_y
6 species (Lee et al., (2009).

7 Figure 2 shows the average diurnal cycle at CVO of measured HONO concentrations. The data
8 exhibits a strong daytime maximum peaking at noon local time (Solar noon ~13:20) and reaching
9 zero at night, indicating a photolytic source. HONO reaches zero at night through deposition,
10 photolysis and reaction with OH suggesting no other surface source causing night time build-up
11 as often is observed otherwise (Ren et al., 2010; VandenBoer et al., 2014; Zhou et al., 2002).

12 Daytime production of HONO is similarly hard to reconcile if its formation by the homogeneous
13 OH + NO reaction (or other gas-phase HO_x-NO_x chemistry, e.g. Li et al., (2014)). With NO
14 mixing ratios below 5 pptV, OH measured peaking at ~ 0.25 pptV during the RHaMBLe
15 campaign (Carpenter et al., 2010; Whalley et al., 2010) and a maximum noontime jHONO of 1.2
16 × 10⁻³ s⁻¹, a steady state HONO mixing ratio of ~ 0.04 pptV is found ($k_{(OH + NO)} = 7.4 \times 10^{-12}$
17 mol.cm⁻³ s⁻¹). An additional source of HONO must be present to explain the observed
18 concentrations.

19 Both the long-term NO_x and the short-term HONO observations made at CVO are difficult to
20 explain with purely gas phase chemistry. Both datasets show daytime maxima indicative of a
21 photolytic source of either NO_x or HONO, whereas gas phase chemistry would predict minima in
22 NO_x during daytime and two orders of magnitude less HONO.

23 **3.2 Box modelling of NO_x sources**

24 Using the box model (section 2.3) we explore the observed diurnal variation in NO_x and
25 understand the role of different processes. Classically, the predominant source of NO_x in remote
26 regions is considered to be the thermal decomposition of compounds such as peroxyacetyl nitrate
27 (PAN) which can be produced in regions of high NO_x and transported long distances (Fischer et



1 al., 2014; Jacobi et al., 1999; Moxim et al., 1996). We consider a source of PAN which descends
2 from the free troposphere and then thermally decomposes to NO_2 in the warm MBL. The main
3 sink of NO_x is conversion to HNO_3 , which is slightly counterbalanced by a slow conversion of
4 HNO_3 back into NO_x through gas phase photolysis or reaction with OH. Figure 3 shows the
5 model with a source of PAN which results in mixing ratios of 5 – 8 pptV, consistent with the few
6 measurements made in the marine boundary layer, most notably by Jacobi et al., (1999) who
7 measured levels from <5 to 22 pptV in the tropical Atlantic, and Lewis et al., (2007) who
8 reported PAN mixing ratios of ~10 pptV in the remote mid-Atlantic MBL.

9 It is evident from the base case model results shown in Fig. 3 that the model fails to calculate the
10 NO_x diurnal cycle. Modelled NO_x concentrations do increase during the night, consistent with
11 the observations, but the model's minimum for NO_x occurs during the day when the observations
12 show a maximum. The modelled and measured HONO is also shown in Fig. 3, both peaking
13 during midday with observations reaching 2.5 pptV whilst the model simulates only ~ 0.2 pptV.
14 It is clear that long-range transport and thermal decomposition of NO_y species such as PAN
15 alone cannot explain the NO_x diurnal at Cape Verde. A PAN-type continuous thermal
16 decomposition forming NO_x would be inconsistent with the diurnal maximum in NO_x which is
17 observed. The NO_x source necessary to support a noon time maximum would have to show a
18 strong day-time maximum to counter the strong diurnal in the sink.

19 This need for a diurnal cycle in the NO_x source also suggests that the shipping source of NO_x is
20 unlikely to explain the diurnal cycle. The dominant source of ship NO_x in the region occurs from
21 the large container ships which pass the region on their way to South America or the Cape of
22 Good Hope. It would appear unlikely that these emissions are systematically higher during the
23 day than during the night and thus are unlikely to explain the observed diurnal signal.

24 There have been a number of papers which have identified much faster photolysis of nitrate
25 within and on aerosol, than for gas phase nitric acid (Baergen and Donaldson, 2013; Cohan et al.,
26 2008; Handley et al., 2007; Ndour et al., 2009; Scharko et al., 2014; Ye et al., 2016a, 2016b;
27 Zhou et al., 2003). These studies have found that particulate nitrate photolysis rates can be up to
28 ~3 orders of magnitude greater than gas phase HNO_3 photolysis in marine boundary layer



1 conditions (Ye et al., 2016b). There is also broad agreement between different studies on the
2 main photolysis product being nitrous acid (HONO) with NO₂ as a secondary species. The
3 product ratio appears dependent on aerosol pH (Scharko et al., 2014). This is shown in reaction
4 (R6) as particulate nitrate (p-NO₃) photolysing to HONO and NO₂ in a ratio $x:y$.



6 There is also evidence that the photolysis rate is positively correlated with relative humidity
7 (Baergen and Donaldson, 2013; Scharko et al., 2014). As such, particulate nitrate photolysis rates
8 appear to increase with increasing aerosol acidity and relative humidity. With the CVO site
9 experiencing relative humidity of 79 % on average (Carpenter et al., 2010) and aerosol
10 containing a significant acidic fraction (Fomba et al., 2014), particulate nitrate photolysis could
11 have a role to play in the NO_x budget at Cape Verde.

12 In order to explore the implications for Cape Verde NO_x chemistry, we re-ran the base model
13 removing the PAN source but including particulate nitrate (p-NO₃) photolysis (R7) leading to
14 HONO and NO₂ production, scaled to the gas phase photolysis of HNO₃. We use an aerosol
15 phase concentration of nitrate of 1.1 μg m⁻³ (equivalent to 400 pptV), which is the mean
16 concentration found in PM10 aerosol at Cape Verde, with little apparent seasonal variability
17 (Fomba et al., 2014). The branching ratio of HONO to NO₂ production from reaction 6 (x and y)
18 was set to 2:1 in line with the findings of Ye et al., (2016b). We scale the p-NO₃ photolysis rate
19 to gas phase HNO₃ photolysis by factors of 1, 10, 25, 50, 100, and 1000. The study of Ye et al.,
20 (2016b) describes enhancements of up to ~300 fold. The impact on the summer months is shown
21 in Fig. 4.

22 Including the photolysis of aerosol nitrate changes both the mean concentration and diurnal cycle
23 of NO_x significantly. The diurnal NO_x is now flat or peaks during the daytime, more consistent
24 with observations. We find the best approximation is achieved when the rate of particulate nitrate
25 photolysis is ~10 times that of HNO₃ which is broadly consistent with laboratory based
26 observations (Zhou et al., 2003). A wide variability of p-NO₃ photolysis rates on different
27 surfaces are reported (Laufs and Kleffmann, 2016; Ye et al., 2016a), thus the photolysis of
28 nitrate is uncertain and likely to be variable with aerosol composition. In all particulate nitrate



1 photolysis-only scenarios, depicted in Fig. 4 and Fig. 5, it is evident that p-NO₃ photolysis alone
2 is doesn't give the observed increase in night time NO_x observations. Conversely the PAN only
3 scenario is insufficient to sustain daytime NO_x. It is therefore likely that the actual source of NO_x
4 is a combination of PAN entrainment from the free troposphere and particulate nitrate photolysis.

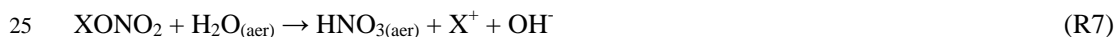
5 Combining the free-tropospheric source of PAN, and the photolysis of particulate nitrate at a rate
6 of 10 times the gas phase HNO₃ photolysis (Fig. 5) results in a model simulation with roughly
7 twice as much NO_x both at night and during daylight but a roughly flat diurnal profile. Simulated
8 HONO peaks at local noon, similar to the observations.

9 3.3 NO_x sinks

10 Figure 6 shows the rates of production and loss analysis for NO_x in this simulation with both
11 PAN thermal decomposition and particulate nitrate photolysis. The largest net source of NO_x
12 after net sinks (such as halogen nitrate cycling) are removed is nitrate (NIT) photolysis to HONO
13 and NO₂. The major net sink is the formation of nitric acid by reaction of NO₂ with OH – though
14 the uptake of HNO₃ onto aerosol and subsequent rapid (compared to gas phase HNO₃) photolysis
15 acts to balance even this.

16 The pronounced drop in modelled NO₂ at sunrise is due to production of halogen nitrates
17 (XONO₂, X = I, Br) when HOX rapidly photolyses to produce XO which can then react with
18 NO₂ to produce XONO₂. XO is formed quickly and spikes in concentration leading to the rapid
19 loss of NO₂. This feature is not observed in the NO_x observations during any season.

20 The diagnostics in Figure 6 show the role of the different sinks of NO_x. In that simulation these
21 are dominated by the gas phase reaction between NO₂ and OH but with the rapid formation and
22 subsequent hydrolysis of BrONO₂ and IONO₂ (R7) playing a major role (Sander et al., 1999).
23 The uptake coefficient (γ) of halogen nitrates onto aerosol therefore could have a strong
24 influence on the NO_x diurnal.





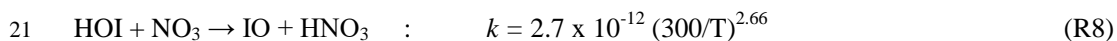
1 We perform a sensitivity analysis on the effect of the uptake coefficients on the NO_x and XO
2 diurnals. We do this in a particulate nitrate photolysis only simulation, without PAN, to isolate
3 the effect of XONO₂ hydrolysis on nitrate-NO_x cycling. Figure 7 shows the effect of changing γ
4 of XONO₂ (X = Br, I) within recommended ranges (Burkholder et al., 2015; Saiz-Lopez et al.,
5 2008) on Saharan dust and sea salt – the predominant aerosol at Cape Verde, ranging from 0.02
6 to 0.8.

7 Increasing the γ of XONO₂ from 0.02 (the low end of recommended values) to 0.1 results in
8 small changes to both the NO_x and XO diurnals. The loss of NO_x at sunrise becomes more
9 pronounced whereas the XO diurnals become slightly more ‘square’ or ‘top-hat’ as per the
10 observations of Read et al., (2008). Increasing the γ to the upper extreme ($\gamma = 0.8$) results in a
11 spike in BrO at sunrise, which consumes the majority of NO₂ though formation of BrONO₂. No
12 combination of uptake coefficients can completely reproduce the characteristic XO diurnals.

13 The effect on the NO_x diurnal of changing γ is clear in that greater uptake coefficients
14 recommended by e.g. JPL (Burkholder et al., 2015) result in objectively worse simulation of both
15 the NO_x and XO diurnals. It is therefore likely that information is lacking from the XO – NO_x
16 chemistry scheme as it is currently known.

17 **3.4 HOI/HOBr - NO_x chemistry**

18 Recently, IO recycling by reaction with NO₃ has been proposed by Saiz-Lopez et al., (2016) who
19 calculated that the reaction (R8) of HOI + NO₃ producing IO and NO₃ has a low enough
20 activation energy and fast enough rate constant to be atmospherically relevant in the troposphere.



22 This mechanism provides a route to nitric acid, and thus particulate nitrate at night, whilst also
23 leading to nocturnal IO production leading to loss of NO₂ by IONO₂ formation.

24 Including this new reaction and re-running the model leads to a diurnal profile of IO much more
25 representative of the observations. This however introduces a more pronounced loss of NO_x at



1 sunrise and sunset, and also results in NO_x peaking during the day which fits better with the
2 observations as shown in Fig. 8.

3 The inclusion of this HOI + NO₃ reaction reproduces the general NO_x and O₃ diurnals more
4 closely than without i.e. a daytime maximum in NO_x. There are also effects on the halogen oxide
5 behaviour. The simulated BrO has a flatter profile, which more closely matches the observations.
6 However, modelled IO is now non-zero at night and the sunrise build-up and sunset decay still
7 occurs more abruptly than the observations.

8 Although the NO_x and O₃ diurnals are reproduced more closely with this new chemistry, there is
9 still disagreement with the observed NO_x diurnal at sunrise and sunset especially indicating a
10 missing reaction or reactions. To best approximate the observed diurnal behaviour an analogous
11 HOBr + NO₃ night time reaction (R9) was introduced with a rate 10 times that of HOI + NO₃ as
12 calculated by Saiz-Lopez et al., (2016).



14 This results in an improved reproduction of the observed NO_x diurnal, Fig. 9. This is a purely
15 speculative representation in order to reproduce the observed NO_x diurnal and highlights how
16 some mechanistic knowledge of NO_x-halogen-aerosol systems is still missing.

17 With HOX + NO₃ chemistry included in the model as in Fig. 9, significant loss of NO_x at sunrise
18 and sunset is eliminated. Greater HONO production is also simulated, with up to ~ 2.5 pptV
19 predicted – in line with the observations shown in Fig. 2. The improvement can be better
20 understood by diagnosing the modelled NO_y distribution. In Fig. 10 the distribution of PAN,
21 IONO₂, BrONO₂, N₂O₅, and NO₃ is shown for the base case scenario (where entrained PAN is
22 the sole source of NO_x in the MBL), for the particulate nitrate photolysis case including HOI +
23 NO₃ chemistry, and the same but also including HOBr + NO₃ chemistry. The major feature
24 changing through the different simulations is the magnitude and shape of the BrONO₂ diurnal.
25 From the base run (A) to the inclusion of HOI + NO₃ chemistry and particulate nitrate photolysis
26 (B) a major increase in BrONO₂ mixing ratio is expected at sun rise and sun set. It is this rapid
27 production of BrONO₂ which consumes NO_x resulting in the sharp dips at these times not seen in



1 the observations. In the HOBr & HOI + NO₃ and particulate nitrate photolysis case (C) these
2 features are eliminated and halogen nitrates do not spike at sunrise or sunset. This leads to a NO_x
3 diurnal which is more representative of the observations. Unsurprisingly, the inclusion of HOX +
4 NO₃ chemistry results in lower mixing ratios of NO₃ at night. In all cases N₂O₅ (in black) is
5 effectively zero at all times.

6 The agreement in modelled and observed NO_x improves and the modelled values fall within the
7 error of the observations. Additionally the approximate BrO diurnal is achieved – without the
8 characteristic ‘horns’, however replicating IO observations is still problematic.

9 The effect of dramatically changing NO_x diurnal could be expected to have an effect on OH and
10 HO₂ mixing ratios. The difference between the base model case, where PAN decomposition is
11 the dominant daytime source, and the final model where the NO_x is more accurately described by
12 particulate nitrate photolysis and HOX + NO₃ chemistry is shown in Fig. 11.

13 In the case of OH the change from the base model to the final model is an increase of 3.3% at the
14 maximum, for HO₂ the increase is a more significant 8.6% (or 1.7 pptV), however this is well
15 within the uncertainty of measured values (Whalley et al., 2010). Figure 11 shows that even with
16 dramatic changes in the NO_x simulation, the OH and HO₂ changes very little comparatively
17 despite increased daytime HONO production.

18 From these simulations it would appear that the photolysis of aerosol phase nitrate may be the
19 dominant source of NO_x into the marine boundary layer around Cape Verde. Particulate nitrate
20 photolysis would be capable of producing a diurnal cycle in NO_x which was consistent with the
21 observations when HOX + NO₃ chemistry is considered also. Whilst agreement between model
22 and observation is improved there is a clear gap in understanding the halogen-NO_x-aerosol
23 system in the remote marine boundary layer.

24 **4 Conclusions**

25 Fast aerosol nitrate photolysis is shown to be likely the primary source of NO_x in the remote
26 tropical Atlantic boundary layer. A 0-D model replicated the observed halogen, O₃, OH, NO_x and
27 HONO levels when including particulate nitrate photolysis at a rate of ~10 times that of gas



1 phase nitric acid, consistent with previous laboratory measurements. Model optimisation shows
2 that this new source of daytime NO₂ is compatible with observations and currently known
3 chemistry at night and at mid-day, but that at sunrise and sunset there is disagreement due to the
4 treatment of halogen oxides at these times. Recently suggested halogen hydroxide + nitrate
5 radical chemistry may provide better agreement between model and observation when theoretical
6 reactions can be substantiated.

7 **Data Availability**

8 We thank the NASA Jet Propulsion Laboratory (Burkholder et al., 2015) for providing
9 comprehensive rate and uptake coefficient data for atmospheric compounds, which can be found
10 at <http://jpldataeval.jpl.nasa.gov>.

11 All data used in this work is available from the British Atmospheric Data Centre (BADC)
12 <http://badc.nerc.ac.uk> and is included as a .csv file in the supplementary information. The
13 DSMACC model is available from <https://github.com/barronh/DSMACC> and a full description
14 of the model can be found in the supplementary information.

15 *Acknowledgements.* The authors would like to thank Luis Neves Mendes of the Instituto
16 Nacional de Meteorologia e Geofísica (INMG) for their operational support at the CVO site. The
17 financial support of NCAS, the National Centre for Atmospheric Science, and of NERC, the
18 Natural Environmental Research Council for supporting the studentship of Chris Reed is
19 gratefully acknowledged. HONO measurements were support by NERC grant NE/M013545/1
20 (Sources of Nitrous Acid in the Atmospheric Boundary Layer).

21 **References**

22 Baergen, A. M. and Donaldson, D. J.: Photochemical renoxification of nitric acid on real urban
23 grime, Environ. Sci. Technol., 47(2), 815–820, doi:10.1021/es3037862, 2013.

24 Beirle, S., Platt, U., von Glasow, R., Wenig, M. and Wagner, T.: Estimate of nitrogen oxide
25 emissions from shipping by satellite remote sensing, Geophys. Res. Lett., 31(18), 4–7,
26 doi:10.1029/2004GL020312, 2004.

27 Burkholder, J. B., Sander, S. P., Abbatt, J., Barker, J. R., Huie, R. E., Kolb, C. E., Kurylo, M. J.,
28 Orkin, V. L., Wilmouth, D. M. and Wine, P. H.: Chemical Kinetics and Photochemical Data for



- 1 Use in Atmospheric Studies, Evaluation No. 18, JPL Publ. 15-10, 15(10), 2015.
- 2 Carpenter, L. J., Fleming, Z. L., Read, K. A., Lee, J. D., Moller, S. J., Hopkins, J. R., Purvis, R.
3 M., Lewis, A. C., Müller, K., Heinold, B., Herrmann, H., Fomba, K. W., Pinxteren, D., Müller,
4 C., Tegen, I., Wiedensohler, A., Müller, T., Niedermeier, N., Achterberg, E. P., Patey, M. D.,
5 Kozlova, E. A., Heimann, M., Heard, D. E., Plane, J. M. C., Mahajan, A., Oetjen, H., Ingham, T.,
6 Stone, D., Whalley, L. K., Evans, M. J., Pilling, M. J., Leigh, R. J., Monks, P. S., Karunaharan,
7 A., Vaughan, S., Arnold, S. R., Tschirner, J., Pöhler, D., Frieß, U., Holla, R., Mendes, L. M.,
8 Lopez, H., Faria, B., Manning, A. J. and Wallace, D. W. R.: Seasonal characteristics of tropical
9 marine boundary layer air measured at the Cape Verde Atmospheric Observatory, *J. Atmos.*
10 *Chem.*, 67(2–3), 87–140, doi:10.1007/s10874-011-9206-1, 2010.
- 11 Carsey, T. P., Churchill, D. D., Farmer, M. L., Fischer, C. J., Pszenny, A. A., Ross, V. B.,
12 Saltzman, E. S., Springer-Young, M., Bonsang, B., Boss, V. B., Saltzman, E. S., Springer-
13 Young, M. and Bonsang, B.: Nitrogen oxides and ozone production in the North Atlantic marine
14 boundary layer, *J. Geophys. Res. Atmos.*, 102(D9), 653–665, doi:10.1029/96JD03511, 1997.
- 15 Cohan, A., Chang, W., Carreras-Sospedra, M. and Dabdub, D.: Influence of sea-salt activated
16 chlorine and surface-mediated renoxification on the weekend effect in the South Coast Air Basin
17 of California, *Atmos. Environ.*, 42(13), 3115–3129, doi:10.1016/j.atmosenv.2007.11.046, 2008.
- 18 Crilley, L. R., Kramer, L., Pope, F. D., Whalley, L. K., Cryer, D. R., Heard, D. E., Lee, J. D.,
19 Reed, C. and Bloss, W. J.: On the interpretation of in situ HONO observations via photochemical
20 steady state, *Faraday Discuss.*, 189(0), 191–212, doi:10.1039/C5FD00224A, 2016.
- 21 Dickerson, R. R., Rhoads, K. P., Carsey, T. P., Oltmans, S. J., Burrows, J. P. and Crutzen, P. J.:
22 Ozone in the remote marine boundary layer: A possible role for halogens, *J. Geophys. Res.*,
23 104(D17), 21,385–21,395, doi:10.1029/1999JD900023, 1999.
- 24 Drummond, J. W., Volz, A. and Ehhalt, D. H.: An optimized chemiluminescence detector for
25 tropospheric NO measurements, *J. Atmos. Chem.*, 2(3), 287–306, doi:10.1007/BF00051078,
26 1985.
- 27 Emmerson, K. M. and Evans, M. J.: Comparison of tropospheric gas-phase chemistry schemes
28 for use within global models, *Atmos. Chem. Phys.*, (1990), 1831–1845, doi:10.5194/acpd-8-
29 19957-2008, 2009.
- 30 Evans, M. J. and Jacob, D. J.: Impact of new laboratory studies of N₂O₅ hydrolysis on global
31 model budgets of tropospheric nitrogen oxides, ozone, and OH, *Geophys. Res. Lett.*, 32(9),
32 L09813, doi:10.1029/2005GL022469, 2005.
- 33 Fischer, E. V., Jacob, D. J., Yantosca, R. M., Sulprizio, M. P., Millet, D. B., Mao, J., Paulot, F.,
34 Singh, H. B., Roiger, A.-E., Ries, L., Talbot, R. W., Dzepina, K. and Pandey Deolal, S.:
35 Atmospheric peroxyacetyl nitrate (PAN): a global budget and source attribution, *Atmos. Chem.*
36 *Phys.*, 14(5), 2679–2698, doi:10.5194/acp-14-2679-2014, 2014.



- 1 Fleming, Z. L., Monks, P. S. and Manning, A. J.: Review: Untangling the influence of air-mass
2 history in interpreting observed atmospheric composition, *Atmos. Res.*, 104–105, 1–39,
3 doi:10.1016/j.atmosres.2011.09.009, 2012.
- 4 Fomba, K. W., Müller, K., Van Pinxteren, D., Poulain, L., Van Pinxteren, M. and Herrmann, H.:
5 Long-term chemical characterization of tropical and marine aerosols at the Cape Verde
6 Atmospheric Observatory (CVAO) from 2007 to 2011, *Atmos. Chem. Phys.*, 14(17), 8883–8904,
7 doi:10.5194/acp-14-8883-2014, 2014.
- 8 Handley, S. R., Clifford, D. and Donaldson, D. J.: Photochemical Loss of Nitric Acid on Organic
9 Films: a Possible Recycling Mechanism for NO_x, *Environ. Sci. Technol.*, 41(11), 3898–3903,
10 doi:10.1021/es062044z, 2007.
- 11 Heland, J., Kleffmann, J., Kurtenbach, R. and Wiesen, P.: A new instrument to measure gaseous
12 nitrous acid (HONO) in the atmosphere, *Environ. Sci. Technol.*, 35(15), 3207–3212,
13 doi:10.1021/es000303t, 2001.
- 14 Jacobi, H.-W.-W., Weller, R., Bluszczyk, T. and Schrems, O.: Latitudinal distribution of
15 peroxyacetyl nitrate (PAN) over the Atlantic Ocean, *J. Geophys. Res.*, 104(D21), 26901–26912,
16 doi:10.1029/1999JD900462, 1999.
- 17 Keene, W. C., Long, M. S., Pszenny, A. A. P., Sander, R., Maben, J. R., Wall, A. J., O'Halloran,
18 T. L., Kerkweg, A., Fischer, E. V. and Schrems, O.: Latitudinal variation in the multiphase
19 chemical processing of inorganic halogens and related species over the eastern North and South
20 Atlantic Oceans, *Atmos. Chem. Phys. Discuss.*, 9(3), 11889–11950, doi:10.5194/acpd-9-11889-
21 2009, 2009.
- 22 Keene, W. C., Stutz, J., Pszenny, A. A. P., Maben, J. R., Fischer, E. V., Smith, A. M., von
23 Glasow, R., Pechtl, S., Sive, B. C. and Varner, R. K.: Inorganic chlorine and bromine in coastal
24 New England air during summer, *J. Geophys. Res.*, 112(D10), D10S12,
25 doi:10.1029/2006JD007689, 2007.
- 26 Kleffmann, J. and Wiesen, P.: Technical note: Quantification of interferences of wet chemical
27 HONO LOPAP measurements under simulated polar conditions, *Atmos. Chem. Phys.*, 8(22),
28 6813–6822, doi:10.5194/acp-8-6813-2008, 2008.
- 29 Laufs, S. and Kleffmann, J.: Investigations on HONO formation from photolysis of adsorbed
30 HNO₃ on quartz glass surfaces, *Phys. Chem. Chem. Phys.*, 18(14), 9616–9625,
31 doi:10.1039/C6CP00436A, 2016.
- 32 Lawler, M. J., Finley, B. D., Keene, W. C., Pszenny, A. A. P., Read, K. A., Von Glasow, R. and
33 Saltzman, E. S.: Pollution-enhanced reactive chlorine chemistry in the eastern tropical Atlantic
34 boundary layer, *Geophys. Res. Lett.*, 36(8), 3–7, doi:10.1029/2008GL036666, 2009.
- 35 Lee, J. D., Moller, S. J., Read, K. A., Lewis, A. C., Mendes, L. and Carpenter, L. J.: Year-round
36 measurements of nitrogen oxides and ozone in the tropical North Atlantic marine boundary layer,



- 1 J. Geophys. Res., 114(D21), D21302, doi:10.1029/2009JD011878, 2009.
- 2 Lewis, A. C., Evans, M. J., Methven, J., Watson, N., Lee, J. D., Hopkins, J. R., Purvis, R. M.,
3 Arnold, S. R., McQuaid, J. B., Whalley, L. K., Pilling, M. J., Heard, D. E., Monks, P. S., Parker,
4 A. E., Reeves, C. E., Oram, D. E., Mills, G., Bandy, B. J., Stewart, D., Coe, H., Williams, P. and
5 Crosier, J.: Chemical composition observed over the mid-Atlantic and the detection of pollution
6 signatures far from source regions, J. Geophys. Res., 112(D10), D10S39,
7 doi:10.1029/2006JD007584, 2007.
- 8 Li, X., Rohrer, F., Hofzumahaus, A., Brauers, T., Haseler, R., Bohn, B., Broch, S., Fuchs, H.,
9 Gomm, S., Holland, F., Jäger, J., Kaiser, J., Keutsch, F. N., Lohse, I., Lu, K., Tillmann, R.,
10 Wegener, R., Wolfe, G. M., Mentel, T. F., Kiendler-Scharr, A. and Wahner, A.: Missing Gas-
11 Phase Source of HONO Inferred from Zeppelin Measurements in the Troposphere, Science (80-
12), 344(6181), 292–296, doi:10.1126/science.1248999, 2014.
- 13 Mahajan, A. S., Plane, J. M. C., Oetjen, H., Mendes, L., Saunders, R. W., Saiz-Lopez, A., Jones,
14 C. E., Carpenter, L. J. and McFiggans, G. B.: Measurement and modelling of tropospheric
15 reactive halogen species over the tropical Atlantic Ocean, Atmos. Chem. Phys., 10(10), 4611–
16 4624, doi:10.5194/acp-10-4611-2010, 2010.
- 17 Monks, P. S., Carpenter, L. J., Penkett, S. A., Ayers, G. P., Gillett, R. W., Galbally, I. E. and
18 Meyer, C. P.: Fundamental ozone photochemistry in the remote marine boundary layer: The
19 SOAPEX experiment, measurement and theory, Atmos. Environ., 32(21), 3647–3664,
20 doi:10.1016/S1352-2310(98)00084-3, 1998.
- 21 Moxim, W. J., Levy, H. and Kasibhatla, P. S.: Simulated global tropospheric PAN: Its transport
22 and impact on NO_x, J. Geophys. Res. Atmos., 101(D7), 12621–12638, doi:10.1029/96JD00338,
23 1996.
- 24 Nakamura, K., Kondo, Y., Chen, G., Crawford, J. H., Takegawa, N., Koike, M., Kita, K.,
25 Miyazaki, Y., Shetter, R. E., Lefter, B. L., Avery, M. and Matsumoto, J.: Measurement of NO₂
26 by the photolysis conversion technique during the Transport and Chemical Evolution Over the
27 Pacific (TRACE-P) campaign, J. Geophys. Res. Atmos., 108(D24), ACH 1-ACH 11,
28 doi:10.1029/2003JD003712, 2003.
- 29 Ndour, M., Conchon, P., D’Anna, B., Ka, O. and George, C.: Photochemistry of mineral dust
30 surface as a potential atmospheric renoxification process, Geophys. Res. Lett., 36(5), L05816,
31 doi:10.1029/2008GL036662, 2009.
- 32 Neu, J. L., Lawler, M. J., Prather, M. J. and Saltzman, E. S.: Oceanic alkyl nitrates as a natural
33 source of tropospheric ozone, Geophys. Res. Lett., 35(13), L13814, doi:10.1029/2008GL034189,
34 2008.
- 35 Pollack, I. B., Lerner, B. M. and Ryerson, T. B.: Evaluation of ultraviolet light-emitting diodes
36 for detection of atmospheric NO₂ by photolysis - chemiluminescence, J. Atmos. Chem., 65(2–3),
37 111–125, doi:10.1007/s10874-011-9184-3, 2011.



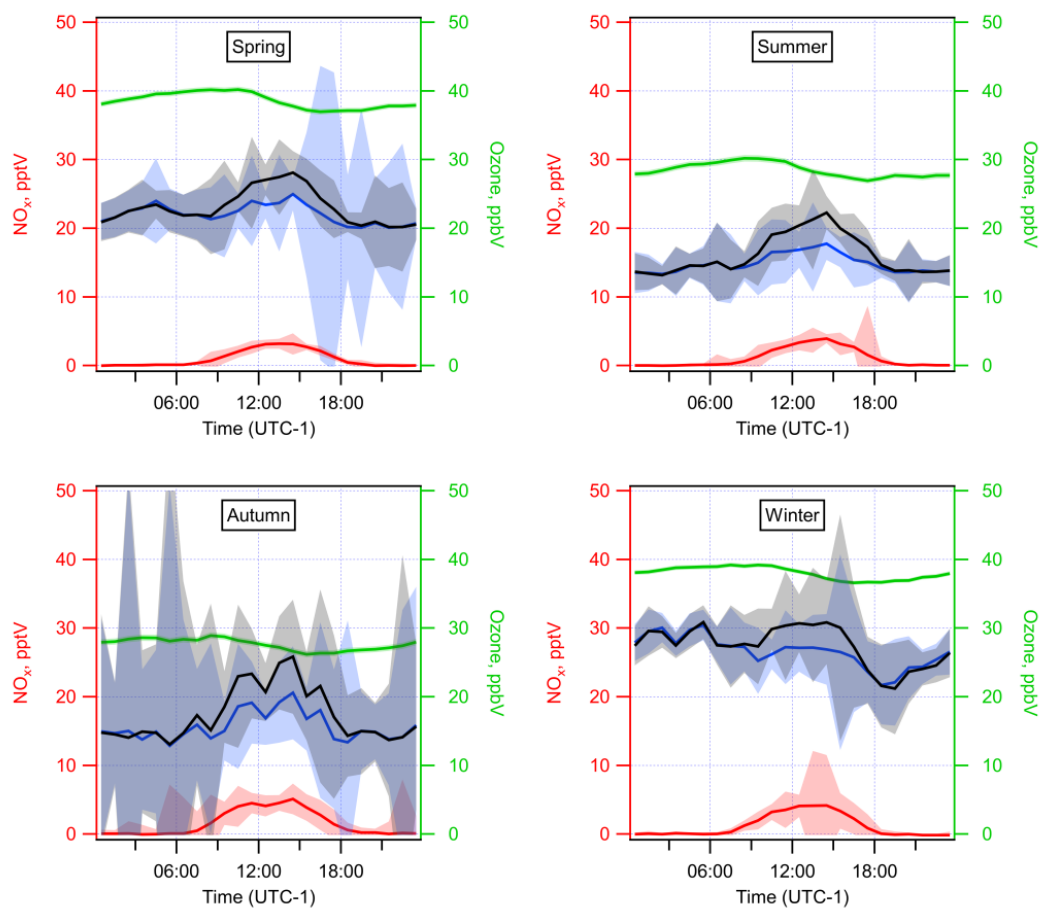
- 1 Pszenny, A. A. P., Moldanová, J., Keene, W. C., Sander, R., Maben, J. R., Martinez, M.,
2 Crutzen, P. J., Perner, D. and Prinn, R. G.: Halogen cycling and aerosol pH in the Hawaiian
3 marine boundary layer, *Atmos. Chem. Phys.*, 4(1), 147–168, doi:10.5194/acp-4-147-2004, 2004.
- 4 Read, K. A., Carpenter, L. J., Arnold, S. R., Beale, R., Nightingale, P. D., Hopkins, J. R., Lewis,
5 A. C., Lee, J. D., Mendes, L. and Pickering, S. J.: Multiannual observations of acetone,
6 methanol, and acetaldehyde in remote tropical atlantic air: implications for atmospheric OVOC
7 budgets and oxidative capacity., *Environ. Sci. Technol.*, 46(20), 11028–39,
8 doi:10.1021/es302082p, 2012.
- 9 Read, K. A., Mahajan, A. S., Carpenter, L. J., Evans, M. J., Faria, B. V. E., Heard, D. E.,
10 Hopkins, J. R., Lee, J. D., Moller, S. J., Lewis, A. C., Mendes, L., McQuaid, J. B., Oetjen, H.,
11 Saiz-Lopez, A., Pilling, M. J. and Plane, J. M. C.: Extensive halogen-mediated ozone destruction
12 over the tropical Atlantic Ocean, *Nature*, 453(7199), 1232–1235, doi:10.1038/nature07035,
13 2008.
- 14 Reed, C., Brumby, C. A., Crilley, L. R., Kramer, L. J., Bloss, W. J., Seakins, P. W., Lee, J. D.
15 and Carpenter, L. J.: HONO measurement by differential photolysis, *Atmos. Meas. Tech.*, 9(6),
16 2483–2495, doi:10.5194/amt-9-2483-2016, 2016a.
- 17 Reed, C., Evans, M. J., Di Carlo, P., Lee, J. D. and Carpenter, L. J.: Interferences in photolytic
18 NO₂ measurements: explanation for an apparent missing oxidant?, *Atmos. Chem. Phys.*, 16(7),
19 4707–4724, doi:10.5194/acp-16-4707-2016, 2016b.
- 20 Ren, X., Gao, H., Zhou, X., Crouse, J. D., Wennberg, P. O., Browne, E. C., LaFranchi, B. W.,
21 Cohen, R. C., McKay, M., Goldstein, A. H. and Mao, J.: Measurement of atmospheric nitrous
22 acid at Blodgett Forest during BEARPEX2007, *Atmos. Chem. Phys.*, 10(13), 6501,
23 doi:10.5194/acp-10-6283-2010, 2010.
- 24 Ridley, D. A., Heald, C. L. and Prospero, J. M.: What controls the recent changes in African
25 mineral dust aerosol across the Atlantic?, *Atmos. Chem. Phys.*, 14(11), 5735–5747,
26 doi:10.5194/acp-14-5735-2014, 2014.
- 27 Ryerson, T. B., Williams, E. J. and Fehsenfeld, F. C.: An efficient photolysis system for fast-
28 response NO₂ measurements, *J. Geophys. Res.*, 105(2), 26,447–26,461,
29 doi:10.1029/2000JD900389, 2000.
- 30 Saiz-Lopez, A., Plane, J. M. C., Cuevas, C. A., Mahajan, A. S., Lamarque, J.-F. and Kinnison, D.
31 E.: Iodine chemistry after dark, *Atmos. Chem. Phys. Discuss.*, 0(June), 1–39, doi:10.5194/acp-
32 2016-428, 2016.
- 33 Saiz-Lopez, A., Plane, J. M. C., Mahajan, A. S., Anderson, P. S., Bauguitte, S. J.-B., Jones, A.
34 E., Roscoe, H. K., Salmon, R. A., Bloss, W. J., Lee, J. D. and Heard, D. E.: On the vertical
35 distribution of boundary layer halogens over coastal Antarctica: implications for O₃, HO_x, NO_x
36 and the Hg lifetime, *Atmos. Chem. Phys.*, 8(4), 887–900, doi:10.5194/acp-8-887-2008, 2008.



- 1 Sander, R., Rudich, Y., von Glasow, R. and Crutzen, P. J.: The role of BrNO₃ in marine
2 tropospheric chemistry: A model study, *Geophys. Res. Lett.*, 26(18), 2857–2860,
3 doi:10.1029/1999GL900478, 1999.
- 4 Scharko, N. K., Berke, A. E. and Raff, J. D.: Release of Nitrous Acid and Nitrogen Dioxide from
5 Nitrate Photolysis in Acidic Aqueous Solutions, *Environ. Sci. Technol.*, 48(20), 11991–12001,
6 doi:10.1021/es503088x, 2014.
- 7 Sherwen, T., Evans, M. J., Carpenter, L. J., Andrews, S. J., Lidster, R. T., Dix, B., Koenig, T. K.,
8 Sinreich, R., Ortega, I., Volkamer, R., Saiz-Lopez, A., Prados-Roman, C., Mahajan, A. S. and
9 Ordóñez, C.: Iodine's impact on tropospheric oxidants: A global model study in GEOS-Chem,
10 *Atmos. Chem. Phys.*, 16(2), 1161–1186, doi:10.5194/acp-16-1161-2016, 2016.
- 11 VandenBoer, T. C., Markovic, M. Z., Sanders, J. E., Ren, X., Pusede, S. E., Browne, E. C.,
12 Cohen, R. C., Zhang, L., Thomas, J., Brune, W. H. and Murphy, J. G.: Evidence for a nitrous
13 acid (HONO) reservoir at the ground surface in Bakersfield, CA, during CalNex 2010, J.
14 *Geophys. Res. Atmos.*, 119(14), 9093–9106, doi:10.1002/2013JD020971, 2014.
- 15 Vogt, R., Sander, R., Von Glasow, R. and Crutzen, P. J.: Iodine chemistry and its role in halogen
16 activation and ozone loss in the marine boundary layer: A model study, *J. Atmos. Chem.*, 32,
17 375–395, doi:10.1023/A:1006179901037, 1999.
- 18 Whalley, L. K., Furneaux, K. L., Goddard, A., Lee, J. D., Mahajan, A., Oetjen, H., Read, K. A.,
19 Kaaden, N., Carpenter, L. J., Lewis, A. C., Plane, J. M. C., Saltzman, E. S., Wiedensohler, A.
20 and Heard, D. E.: The chemistry of OH and HO₂ radicals in the boundary layer over the tropical
21 Atlantic Ocean, *Atmos. Chem. Phys.*, 10(4), 1555–1576, doi:10.5194/acp-10-1555-2010, 2010.
- 22 Ye, C., Gao, H., Zhang, N. and Zhou, X.: Photolysis of Nitric Acid and Nitrate on Natural and
23 Artificial Surfaces, *Environ. Sci. Technol.*, acs.est.5b05032, doi:10.1021/acs.est.5b05032, 2016a.
- 24 Ye, C., Zhou, X., Pu, D., Stutz, J., Festa, J., Spolaor, M., Tsai, C., Cantrell, C., Mauldin, R. L.,
25 Campos, T., Weinheimer, A., Hornbrook, R. S., Apel, E. C., Guenther, A., Kaser, L., Yuan, B.,
26 Karl, T., Haggerty, J., Hall, S., Ullmann, K., Smith, J. N., Ortega, J. and Knote, C.: Rapid
27 cycling of reactive nitrogen in the marine boundary layer, *Nature*, 532(7600), 489–491,
28 doi:10.1038/nature17195, 2016b.
- 29 Zhou, X., Civerolo, K., Dai, H., Huang, G., Schwab, J. and Demerjian, K.: Summertime nitrous
30 acid chemistry in the atmospheric boundary layer at a rural site in New York State, *J. Geophys.*
31 *Res. Atmos.*, 107(D21), ACH 13-1-ACH 13-11, doi:10.1029/2001JD001539, 2002.
- 32 Zhou, X., Gao, H., He, Y., Huang, G., Bertman, S., Civerolo, K. and Schwab, J.: Nitric acid
33 photolysis on surfaces in low-NO_x environments: significant atmospheric implications,
34 *Geophys. Res. Lett.*, 30(23), ASC 12/1--ASC 12/4, doi:10.1029/2003GL018620, 2003.



1

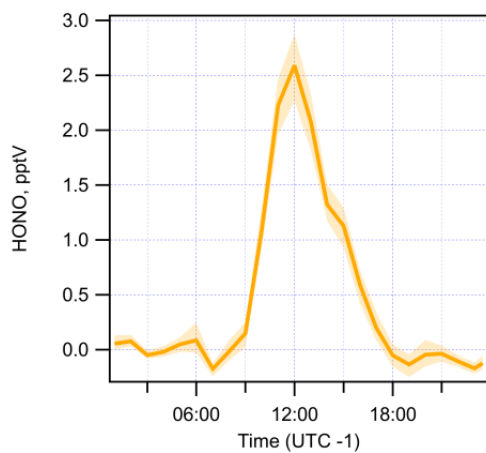


2

3 Figure 1. The observed seasonal diurnal cycles in NO, NO₂, NO_x, and O₃ at the CVO GAW
4 station during 2014 and 2015. NO is shown in red, NO₂ in blue, NO_x in black, and O₃ in green.
5 Shaded areas indicate the standard error of data.

6

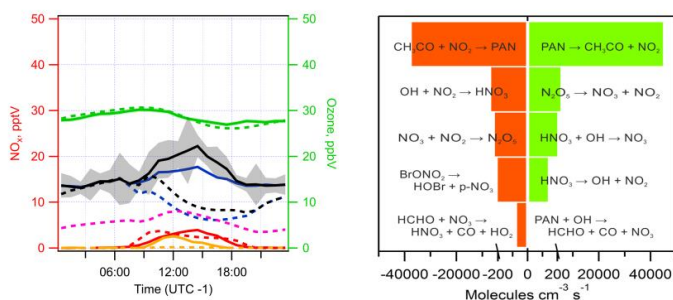
7



1

2 Figure 2. The observed average HONO diurnal measured at CVO during 24th November – 3rd
3 December 2015. Shaded area indicates standard deviation of data.

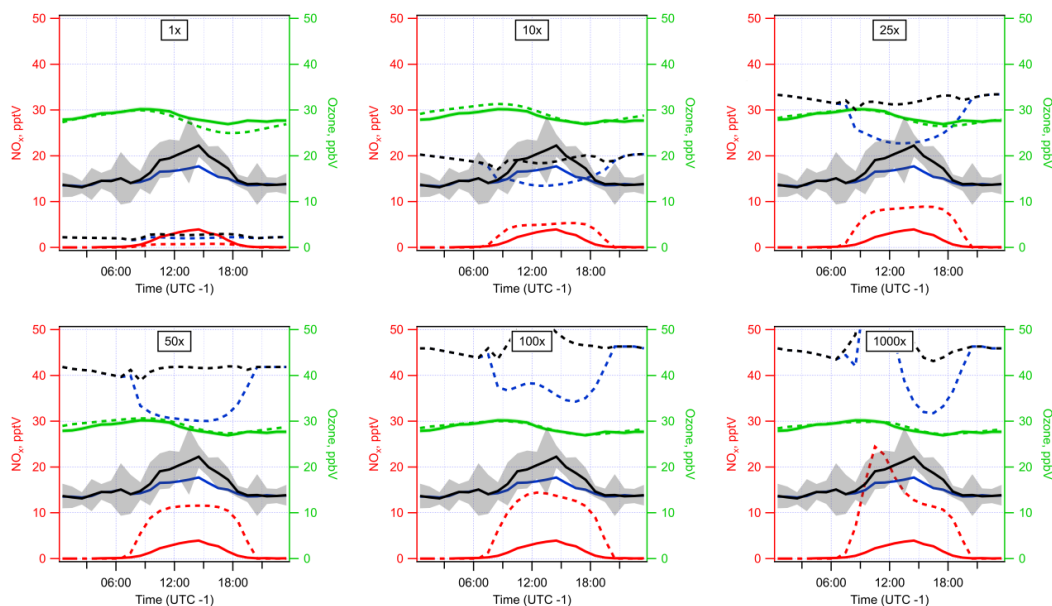
4



1

2 Figure 3. Left shows the measured (solid lines) and modelled (dashed) NO_x and HONO diurnal
 3 behaviour at the CVO GAW station where the dominant source of NO_x is a source of PAN
 4 descending from the upper troposphere having been transported from polluted regions. O₃ –
 5 green; NO_x – black; NO₂ – blue; NO – red; HONO – yellow; PAN – pink. Right shows the rates
 6 of production and loss of NO and NO₂ from sources listed in descending order of contribution
 7 over a 24 hour period accounting for >95% of the total. Shaded areas are standard error of the
 8 observation.

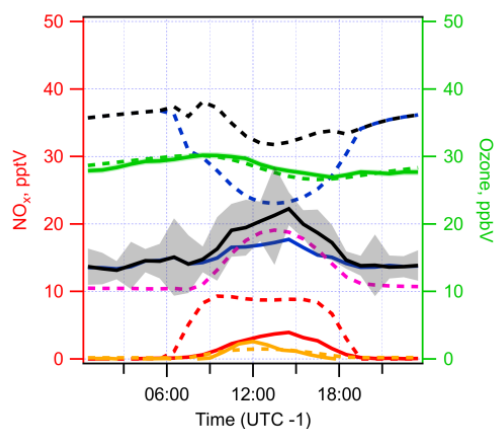
9



1

2 Figure 4. The modelled diurnal profile of NO_x at CVO during summer months when photolysis
3 of nitrate is considered. The rate of particulate nitrate photolysis has been scaled to the rate of
4 HNO_3 photolysis by factors of 1, 10, 25, 50, 100, and 1000. Observations are solid lines whilst
5 modelled values are shown dashed. Shaded areas are standard error of the observation. O_3 –
6 NO_x – black; NO_2 – blue; NO – red.

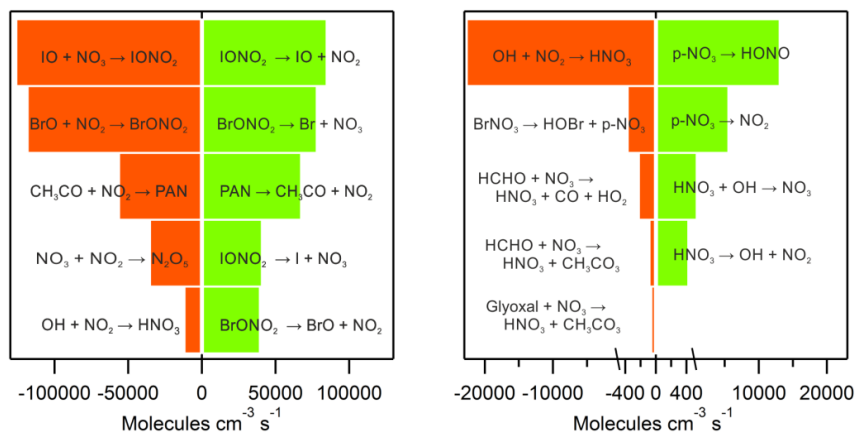
7



1

2 Figure 5. The modelled diurnal profile of NO_x at CVO during summer months when photolysis
3 of nitrate (set at $10\times$ the gas phase HNO_3 photolysis) and a tropospheric PAN source are
4 considered. Shaded areas for NO_x are the standard error of the observation. O_3 – green; NO_x –
5 black; NO_2 – blue; NO – red; HONO – yellow; PAN – pink.

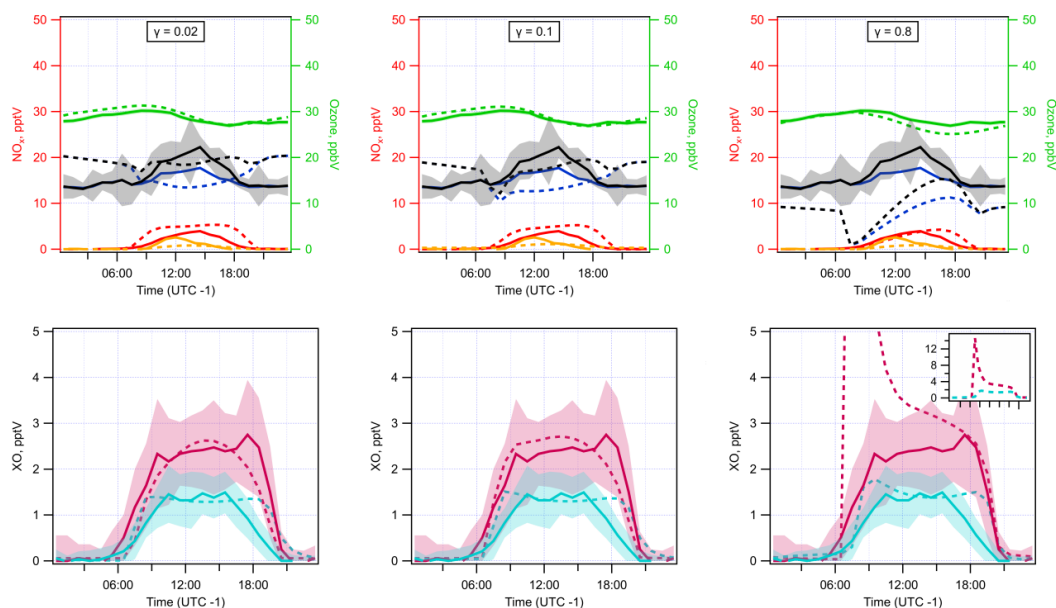
6



1

2 Figure 6. Left is the production and loss analysis of the combined model of particulate nitrate
 3 photolysis and PAN decomposition over 24 hours. Right is the same analysis discarding the
 4 major balanced sinks of fast cycling short lived species.

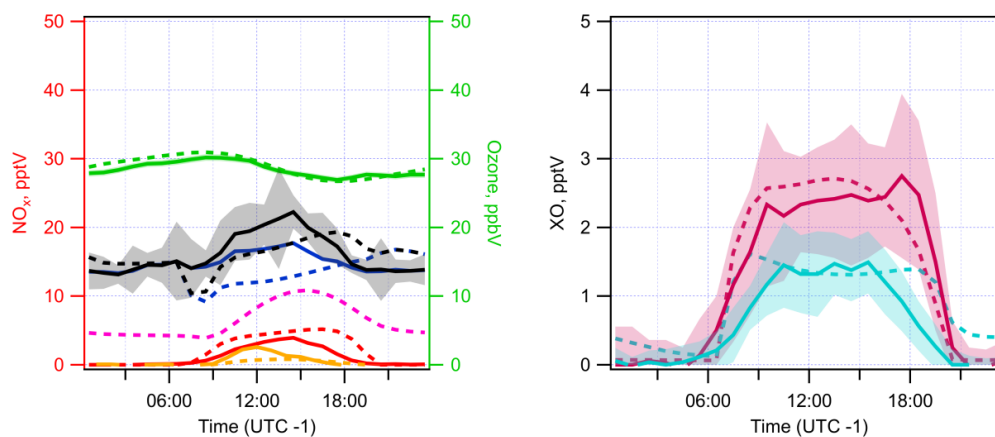
5



1

2 Figure 7. Sensitivity analysis of the effect of changing reactive uptake co-efficients (γ) of
3 reactive halogens (XO, XHO, XONO₂, X = Br, I) on NO_x (top) and XO (bottom) diurnal
4 behaviour during summer months at CVO. Particulate nitrate photolysis is set at 10 times the rate
5 of gaseous HNO₃. Observations are solid lines whilst modelled values are shown as dashed. IO
6 and BrO observations are adapted from Read et al., (2008). Shaded areas are standard error of
7 the observation. O₃ – green; NO_x – black; NO₂ – blue; NO – red; HONO – yellow; PAN – pink;
8 IO – turquoise; BrO – purple.

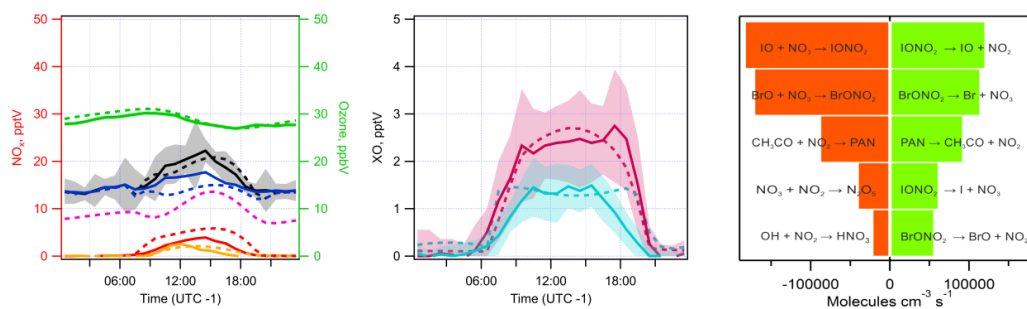
9



1

2 Figure 8. Left is the modelled NO_x and HONO diurnal cycle for the CVO site during summer
3 months with the inclusion of night time HOI chemistry. Centre is the observed (adapted from
4 Read et al., (2008)) and modelled IO and BrO. Observations are solid lines whilst modelled
5 values are shown dashed. Shaded areas are standard error of the observation. O₃ – green; NO_x –
6 black; NO₂ – blue; NO – red; HONO – yellow; PAN – pink; IO – turquoise; BrO – purple.

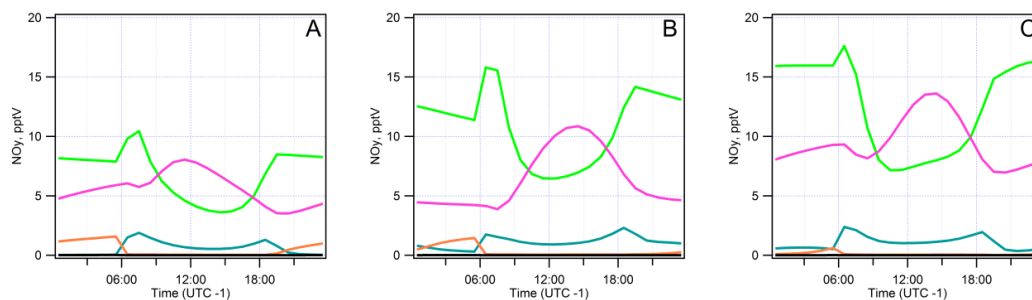
7



1

2 Figure 9. NO_x and halogen oxide diurnals for the CVO site during summer months. Observations
 3 are solid lines (BrO and IO adapted from Read et al., (2008)) whilst modelled values are shown
 4 dashed. Shaded areas are standard error of the observation. O_3 – green; NO_x – black; NO_2 – blue;
 5 NO – red; HONO – yellow; PAN – pink; IO – turquoise; BrO – purple. Night-time $\text{HOI} + \text{NO}_3$
 6 chemistry is included as is speculative HOBr chemistry analogous to that of HOI .

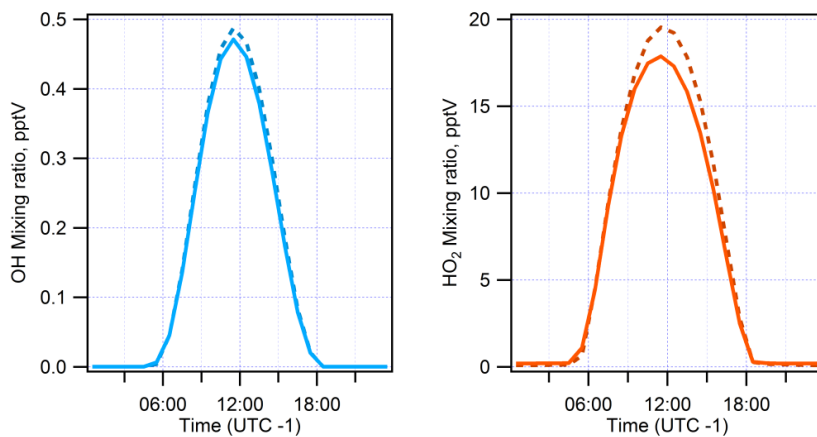
7



1

2 Figure 10. Shown are NO_y diurnals for the CVO site during summer months in the base scenario
 3 (A), with HOI + NO₃ chemistry included (B), and with HOI & HOBr + NO₃ chemistry included
 4 (C). BrONO₂ = green, IONO₂ = teal, PAN = pink, NO₃ = orange, N₂O₅ = black.

5



1

2 Figure 11. Modelled OH (left) and HO₂ (right) mixing ratios comparing the base case model
3 where PAN decomposition is the dominant source of NO_x in the remote MBL (solid lines), with
4 the final model where the dominant source of NO_x is particulate nitrate photolysis and HOX +
5 NO₃ chemistry is included.

6